Am J Transl Res 2020;12(9):5538-5550
www.ajtr.org /ISSN:1943-8141/AJTR0111113

Original Article

Oxymatrine inhibits the development of non-small cell lung cancer through miR-367-3p upregulation and target gene *SGK3* downregulation

Qinghua Yu[1*], Jiewei Luo[2*], Jiguang Zhang[3], Yangming Chen[3], Kai Chen[3], Jianbin Lin[3], Shihui Sun[3], Xing Lin[3]

[1]Department of Radiology, Fujian Provincial Hospital, Provincial Clinical College of Fujian Medical University, Fuzhou, Fujian, China; [2]Department of Traditional Chinese Medicine, Fujian Provincial Hospital, Provincial Clinical College of Fujian Medical University, Fuzhou, Fujian, China; [3]Department of Thoracic Surgery, Fujian Provincial Hospital, Provincial Clinical College of Fujian Medical University, Fuzhou, Fujian, China. [*]Equal contributors.

Received March 19, 2020; Accepted July 22, 2020; Epub September 15, 2020; Published September 30, 2020

Abstract: Oxymatrine (OM), an important active ingredient extracted from *sophora flavescens*, has attracted more attention for its anti-tumor effect in recent years, with pronounced effects on the development of multiple tumors, acting as a potential effective low toxic drug in clinical tumor treatment. In this study, CCK-8 and transwell experiments were applied to detect cell proliferation and migration. Quantitative real-time polymerase chain reaction (qRT-PCR) and Western blotting were used to test the expression of miR-367-3p and serum and glucocorticoid regulated kinase 3 (*SGK3*). The function of oxymatrine in non-small cell lung cancer (NSCLC) progression was also confirmed *in vivo*. Then, CCK-8 and transwell assays revealed that oxymatrine could repress NSCLC cell migration and proliferation. qRT-PCR showed the striking promotion roles of oxymatrine in cancer suppressor gene miR-367-3p expression. The results of further dual luciferase reporter gene experiment demonstrated that *SGK3* was a target gene of miR-367-3p and under the regulation of oxymatrine. The rescue experiments indicated that OM functioned via miR-367-3p, while miR-367-3p exerted its function by action on *SGK3*. Finally, *in vivo* studies showed that OM could also inhibit tumor growth. As a result, this study found that OM inhibited the development of NSCLC through reducing the expression of a downstream target gene *SGK3* by promoting miR-367-3p expression.

Keywords: Non-small cell lung cancer, oxymatrine, miR-367-3p, *SGK3*

Introduction

In recent decades, lung cancer incidence and mortality have been overtly increased and it has become a major cause of death around the world. Non-small cell lung cancer (NSCLC), as the most prevalent cancer, accounts for about 85% of all kinds of lung cancers [1]. The 5-year survival rate of NSCLC is still low, albeit the great progress in the diagnosis method, surgical technique, and the new lung cancer chemotherapy regimen in recent years [2, 3]. Therefore, it is of great importance to explore more effective therapeutic methods.

Oxymatrine (OM) is a natural alkaloid of tetracyclic quinolizidines, mainly extracted and purified from *sophora flavescens*. Oxymatrine is used for tumor diseases in clinical settings for its anti-inflammatory, analgesic effects, virus resistance, immunoregulation promotion, and prevention of arrhythmia and infection. In some studies, *in vivo* and *in vitro* experiments indicate that oxymatrine may suppress the proliferation of prostatic cancer cells while its Western blot analysis shows significantly higher expressions of p53 and bax, and a strikingly lower bcl-2 expression under the action of oxymatrine [4]. In addition, other studies suggest that oxymatrine activates caspase-3 and bax and downregulates the expressions of bcl-2 and nuclear factor NF-κB to suppress the proliferation of gallbladder cancer cells [5]. However, some studies find that after oxymatrine intervenes in human lung cancer cells (A549) and human breast cancer cells (MCF-7), oxymatrine induces the apoptosis of these cells and its mechanism is associated with the enhanced

expression of bax and caspase-3 proteins, and with a lower expression of bcl-2 proteins [6, 7]. Thus, it can be seen that oxymatrine exerts inhibitory roles in several tumors by virtue of tumor cell proliferation inhibition, cell apoptosis induction, cell cycle blocking, cell invasion and metastasis suppression, and assistance in the synergism and attenuation of chemoradiotherapy, thereby exhibiting a good clinical application prospect. It is necessary to further explore of the roles and possible mechanisms of oxymatrine in NSCLC, albeit the increasing studies on the anti-tumor effects and the mechanism of oxymatrine.

MicroRNAs (miRNAs), a class of non-coding single stranded RNAs with about 22 nucleotides, have regulatory effects on target gene expression via binding to downstream target genes. Studies have proven that miRNAs are intimately intertwined with the development of multiple tumors and it is widely involved in tumors [8, 9]. The results of previous studies have showed that miR-367-3p plays a certain role in multiple tumors. For instance, overexpressed microRNA-367-3p suppresses the invasion and proliferation of cervical cancer cells by downregulating SPAG5-mediated Wnt/β-catenin signaling [10]. A study has demonstrated that miR-367-3p is a serum biomarker in metastatic testicular germ cell cancer before, during, and after chemotherapy [11]. However, a study has also found that PIWIL3/OIP5-AS1/miR-367-3p/CEBPA feedback loop presents regulatory effects on biological characteristics of glioma cells [12]. Nevertheless, there is no report on the research of miR-367-3p in NSCLC.

In this study, in the oxymatrine treated NSCLC cell lines, cell proliferation and migration were remarkably inhibited and miR-367-3p expression was notably increased, accordingly. Therefore, the objectives of this study were to explore the functions of oxymatrine in the occurrence and development of NSCLC and further elucidate its possible mode of action.

Materials and methods

Cell culture

The cell bank of the Chinese academy of sciences provided the NSCLC cell lines H1299 and A549. The cells were cultured in Roswell Park Memorial Institute (RPMI) 1640 medium (GIBCO-BRL; Thermo Fisher Scientific, Waltham, MA, USA) with 10% of fetal bovine serum (FBS; Hyclone, USA) in a constant temperature incubator with 5% CO_2 and saturated humidity at 37°C.

Cell transfection

After seeding appropriate cells into a 6-well plate, cells were cultured in antibiotic-free medium and subjected to transient transfection until 60-70% of the culture dish was covered by cells. Cells were transfected with miR-367-3p inhibitor/mimics, *SGK3* siRNA/pcDNA3.1, and paired with a negative control, followed by mixing with lipo2000. Then, a complex was formed after 20 min of homogenization at room temperature, 100 μL of this complex were slowly added into the medium for mixing. After 4-6 h of co-culture, this complex was replaced by complete medium with 10% FBS and 1% streptomycin/penicillin for 24 h of culture for subsequent experiments.

Cell proliferation assay

Cell counting kit-8 assay (CCK-8, Dojin, Japan) was used to determine the proliferation of A549 and H1299 cells. Transfected cells were seeded into a 96-well plate at 2,000 cells/well. Seventy-two hours later, 10 μL of CCK-8 solution were dropped into each well, followed by 2 h of incubation at 37°C. The absorbance was measured using a SpectraMax M5 microplate reader (Molecular Devices) at 450 nm.

Colony formation assay

After transfection, cells were seeded in a 12-well plate and cultured for 15 days in complete medium. Cells were then subjected to methanol fixation and 0.1% crystal violet staining (Sigma-Aldrich). Finally, a microscope was used to count the colonies containing at least 50 cells.

Transwell assay

An *in vitro* cell migration assay was performed using 24-well chambers with an 8 μm pore size (Corning). Cells were re-suspended in 100 μL of serum-free medium at a concentration of 10^5 cells/mL. Subsequently, for the cell migration and invasion assay, cells were seeded in the upper chamber, while 600 μL of 10% FBS medi-

um were added to the lower chamber. A cotton swab was used for wiping off cells on the upper membrane surface after 48 h of incubation. Cells that migrated to the lower membrane side were fixed in methanol, followed by 10% Giemsa staining. Five fields were randomly selected under a microscope for cell counting and statistical analyses, and photos were taken.

Quantitative RT-PCR (qRT-PCR) analysis

Trizol reagent (Life Technologies Corporation, Carlsbad, CA) was utilized for the extraction of total RNAs from glioma cells and tissues, and a Nanodrop Spectrophotometer (ND-100, Thermo, Waltham, MA) was utilized for detecting RNA concentration and quality at 260/280 nm. The primers and cDNA from miRNA were synthesized using Thermo Fisher and TaqMan miRNA Reverse Transcription kit (Thermo Fisher), respectively. One-Step SYBR PrimeScript RT-PCR Kit (Perfect Real Time, RR066A) (Takara Bio., Inc., Japan) was used for qRT-PCR. In the ABI 7500 Fast Real-Time PCR System (Applied Biosystems), TaqMan microRNA assays of U6 and miR-367-3p (Applied Biosystems) were carried out using TaqMan Universal Master Mix II. With expressions standardized to endogenous control, the fold change was obtained using the relative quantification ($2^{-\Delta\Delta Ct}$) method. The primers used are listed below: *SGK3,* F: 5'-CAGGCTGTAAGACTCACTCC-3', R: 5'-TTGCTATTTCTGACACCACTA-3'; GAPDH, F: 5'-AGAAGGCTGGGGCTCATTTG-3', R: 5'-AGGGGCCATCCACAGTCTTC-3'.

Luciferase reporter gene assay

After construction of *SGK3*-3'UTR-mut and *SGK3*-3'UTR-wt plasmids and 24 h prior to transfection, cells were uniformly seeded onto a 24-well plate at 5×10^4 cells/mL. Lip2000 was added according to the instructions of Lipofectamine™ 2000 together with pRL-TK (20 ng) and luciferase reporter vector (400 ng) at 80% of cell confluence and in good cell state, followed by cell culture in an incubator with 5% CO_2 at 37°C. Twenty-four hours later, with the medium discarded, cell washing was performed once using ice PBS. To dissolve the cells, after the addition of 100 μL of PBS, cells were shaken at 150 rpm on a shaker at room temperature for 20 min. After the chemiluminescence apparatus was started, 20 μL of LAR II solution and 20 μL of the above cell lysis buffer were successively added into the measuring tube for homogeneous mixing. Subsequently, the fluorescence intensity (FI) of luciferase reporter system was measured. For the measurement of the FI internal reference (Renilla luciferase), 20 μL of Stop & Glo stop buffer were placed into the reaction tube for another measurement after detection. The FI of the reporter gene (internal reference) was utilized for the calculation of the relative expression abundance of the reporter gene.

Western blotting

RIPA buffer with 1 mM EDTA (pH 8.0) and 50 mM HEPES was used for extracting the total protein from frozen cells on ice. A bicinchoninic acid (BCA) protein assay kit (Beyotime, Shanghai, China) was utilized for determining the protein concentration of supernatant extracts. Samples were subjected to sodium dodecyl sulfate-polyacrylamide gel electrophoresis and electrophoretically transferred onto a PVDF membrane. Subsequently, the membrane was incubated in tris-buffered saline with 5% nonfat milk at room temperature for 2 h, and then incubated with primary antibodies (SGK3, ab126108, abcam. β-catenin, #8814, CST. GAPDH, ab181602, and abcam) for 18 h. Incubation with a paired secondary antibody (Santa Cruz, Dallas, TX) was done for 2 h. Enhanced chemiluminescence (ECL kit, Beyotime, Shanghai, China) was used for observing the immunoblots and ChemImager 5,500 V2.03 software (Alpha Innotech, San Leandro, CA) was utilized for their scanning. The relative integrated density value was calculated using GAPDH as an internal control.

Preparation of tumor-bearing mouse model

The oxymatrine-treated (50 and 100 μM) and untreated (control) groups were constructed by adjusting the density of logarithmically grown A549 cells to 1×10^6 cells/mL by using 100 μL of DMEM medium. Before counting, cells were re-suspended into individual cells using PBS. The tumor was placed at the bilateral rumps of each nude mouse on the clean bench until living cells accounted for over 90%. Pimples might form at the injection site. The oxymatrine-treated group was subjected to treatment using 50 and 100 μM Oxymatrine for 7 days. A seven-day interval was used for measuring tumor size. Mice were euthanatized

at 28 days to take tumors for measurement and weighing. The tumor volume was calculated as volume = length × width × height × 0.5. Tumor growth curves were drawn.

Immunohistochemical staining

The tumor tissues were placed into a 10% neutral formalin solution with five times the tumor volume to fix them for 24 h. The necrotic parts of fixed tissues were trimmed at about 5 mm of thickness, followed by dehydration, permeabilization, and waxing in an embedding box. These treated tissues were embedded in an embedding mold for further application. Waxes were trimmed and cut into 4-μm-thick slices using a slicer, and then flattened and patched for 2 h, by baking them at 60°C. Before any immunohistochemical analysis and post dewaxing, staining, dehydration, permeabilization, and mounting, a reference immunohistochemistry kit (streptavidin-perosidase, SP method) was used for further experiments.

Statistical analysis

All the statistical analyses were conducted by using SPSS 18.0 statistical software (IBM, New York, NY, USA). For normally distributed data with equal variance, the difference was evaluated by 2-tailed Student t test (2-group comparisons) or ANOVA followed by the post hoc Bonferroni test (multigroup comparisons) as appropriate. For nonnormally distributed data or data with unequal variances, the difference was evaluated by a nonparametric Mann-Whitney U test (2-group comparisons) or the Kruskal-Wallis test followed by the post hoc Bonferroni test (multigroup comparisons). The data are presented as mean ± standard error of the mean (SEM). $P < 0.05$ was considered statistically significant.

Results

OM inhibited NSCLC cell proliferation and migration

Firstly, cell lines A549 and H1299, which were commonly utilized in NSCLC studies, were used in this experiment to detect whether OM participated in the progression of NSCLC cells. Different concentrations of OM and NSCLC cells were used in incubation for the detection of cell proliferation of each group based on a CCK-8 assay after 24 h. The detection revealed a concentration-dependent gradual decrease in cell proliferation with a lower OM concentration (**Figure 1A**, **1B**). In subsequent experiments, a 50 μM concentration was selected as the treatment concentration. Based on the CCK-8 assay results at 24 h intervals for three consecutive days, OM could significantly inhibit the proliferation of NSCLC cells (**Figure 1C**, **1D**). Meanwhile, a plate cloning experiment was also conducted and indicated that the cell clone number in OM-treated group was also considerably lower, in comparison with the control group (**Figure 1E**). A transwell experiment was used for detecting the roles of OM in cell migration and showed a notable decrease in the migration of OM incubated NSCLC cells (**Figure 1F**).

OM promoted miR-367-3p expression

After treating the cells using OM at different concentrations, qRT-PCR was conducted for detecting miR-367-3p expression in cells of each group and revealed a significantly high expression of miR-367-3p post OM stimulation in a dose-dependent manner, relative to untreated cells (**Figure 2A**). To determine whether miR-367-3p had any effect on NSCLC cell proliferation and migration, miR-367-3p mimics and their negative controls were transfected with A549 and H1299 cells for transfection efficiency detection, and the results revealed a significant increase in miR-367-3p expression (**Figure 2B**). Subsequently, the CCK-8 assay suggested that the upregulated miR-367-3p expression considerably reduced the proliferation of A549 and H1299 cells, relative to the control group (**Figure 2C**, **2D**), as demonstrated by using a plate cloning experiment (**Figure 2E**). Meanwhile, during the transwell experiment, the migration of A549 and H1299 cells was also notably inhibited after upregulation of miR-367-3p (**Figure 2F**).

SGK3 was a target gene of miR-367-3p

Based on bioinformatics analysis, *SGK3* was a possible target of miR-367-3p and possible binding sites existed between them (**Figure 3A**), as demonstrated by the dual luciferase reporter gene experiment (**Figure 3B**). *SGK3* expression was measured in A549 and H1299 cells with an miR-367-3p upregulation for further verification. The results uncovered that post

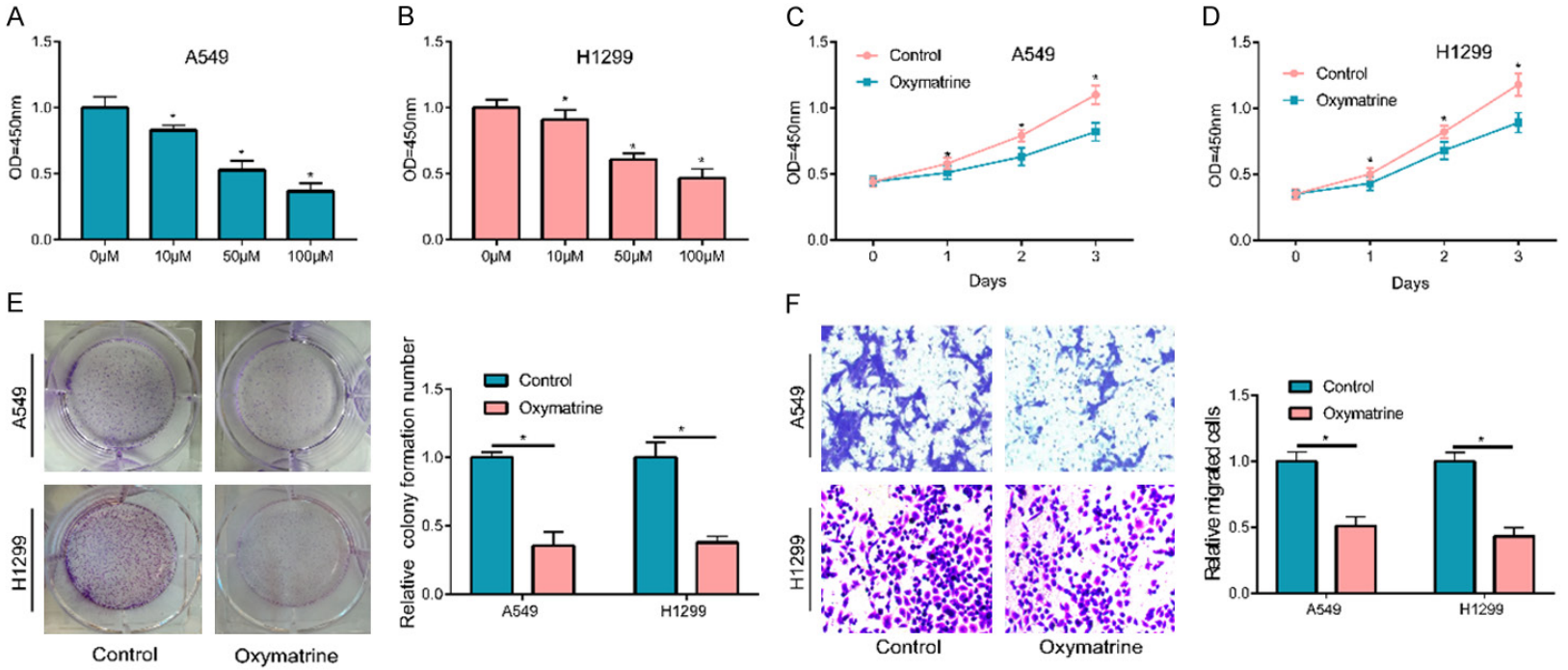

Figure 1. OM inhibited NSCLC cell proliferation and migration. (A, B) Treated with 10, 50 and 100 μM OM for 24 h, A549 and H1299 cells' proliferation were inhibited and has a certain concentration effect. 50 μM concentration was selected for subsequent study. When cells treated with 50 μM OM, the cell proliferation (C, D) cell colony formation (E) and cell migration (F) was faded obviously. *(*P < 0.05).*

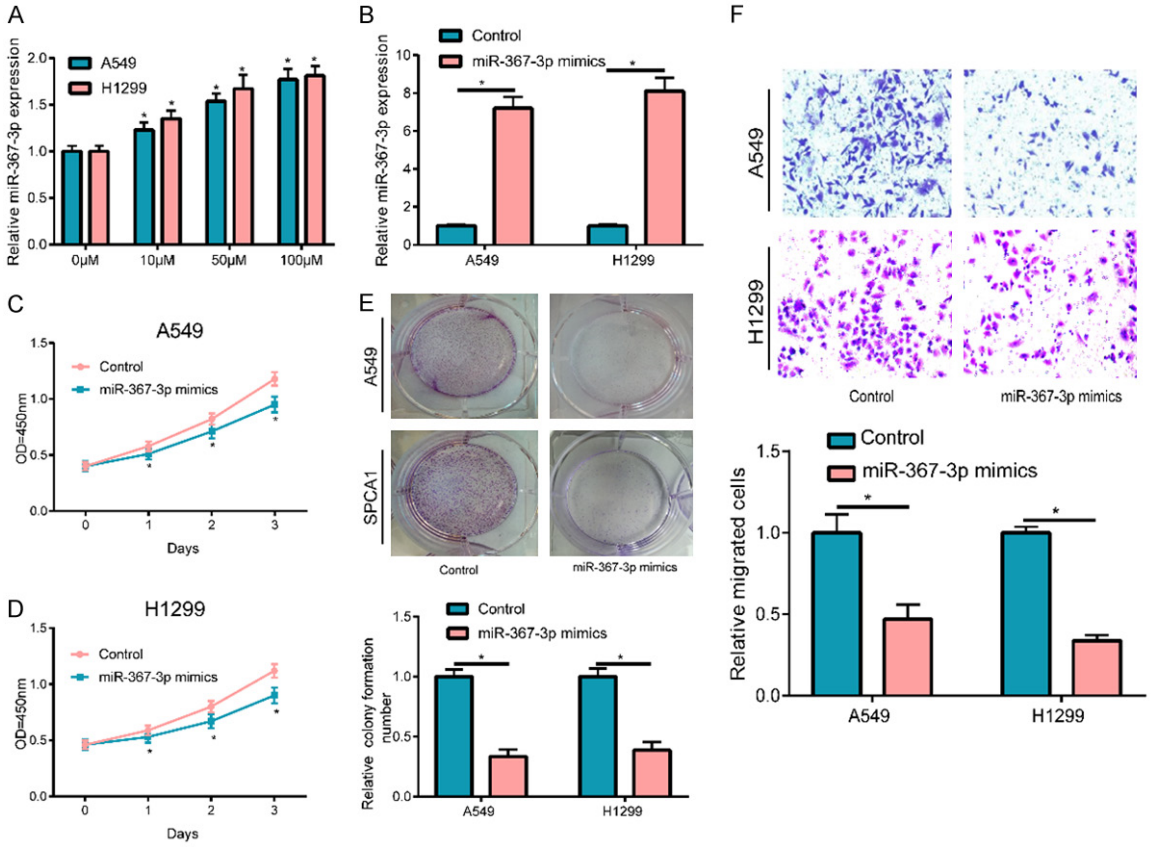

Figure 2. OM promoted miR-367-3p expression. A. After treated with 10, 50 and 100 μM OM, miR-367-3p expression was up-regulated in concentration-dependent pattern in A549 and H1299 cells. B. Post transfection of A549 and H1299 cells using miR-367-3p mimics, miR-367-3p was up-regulated apparently. C-E. The upregulation of miR-367-3p significantly suppressed cell proliferation and clone in A549 and H1299 cells. F. Cell migration was notably suppressed by overexpressing miR-367-3p. *(*P < 0.05).*

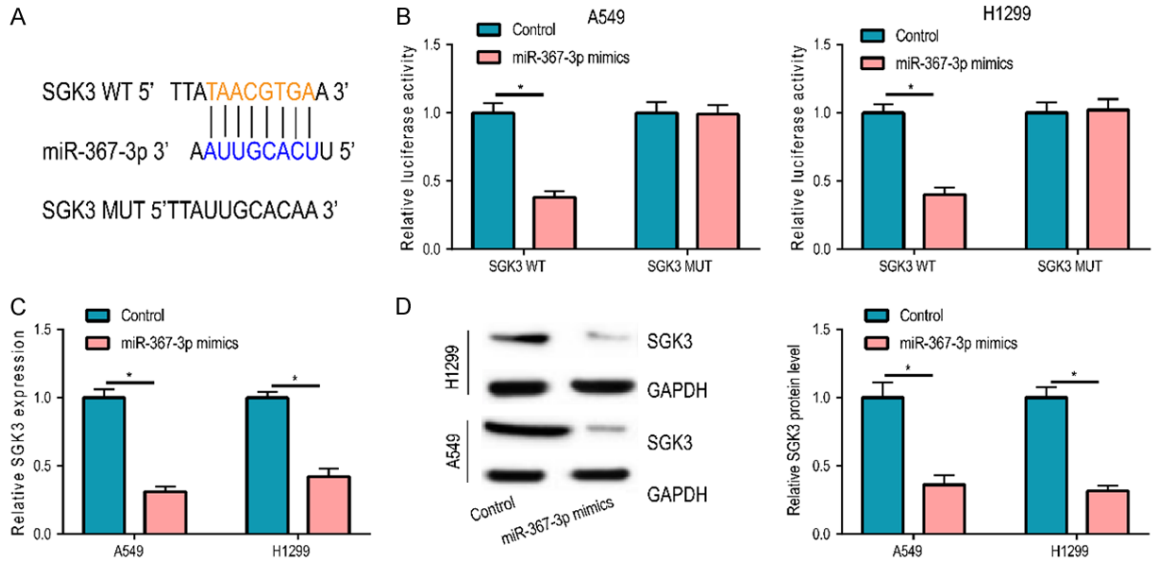

Figure 3. *SGK3* was a target gene of miR-367-3p. A. miR-367-3p and *SGK3* existed possible binding sites. B. Dual luciferase reporter gene experiment confirmed the combination relationship between miR-367-3p and *SGK3*. C, D. After upregulation of miR-367-3p expression in A549 and H1299 cells, the mRNA and protein levels of *SGK3* were significantly reduced. *(*P < 0.05).*

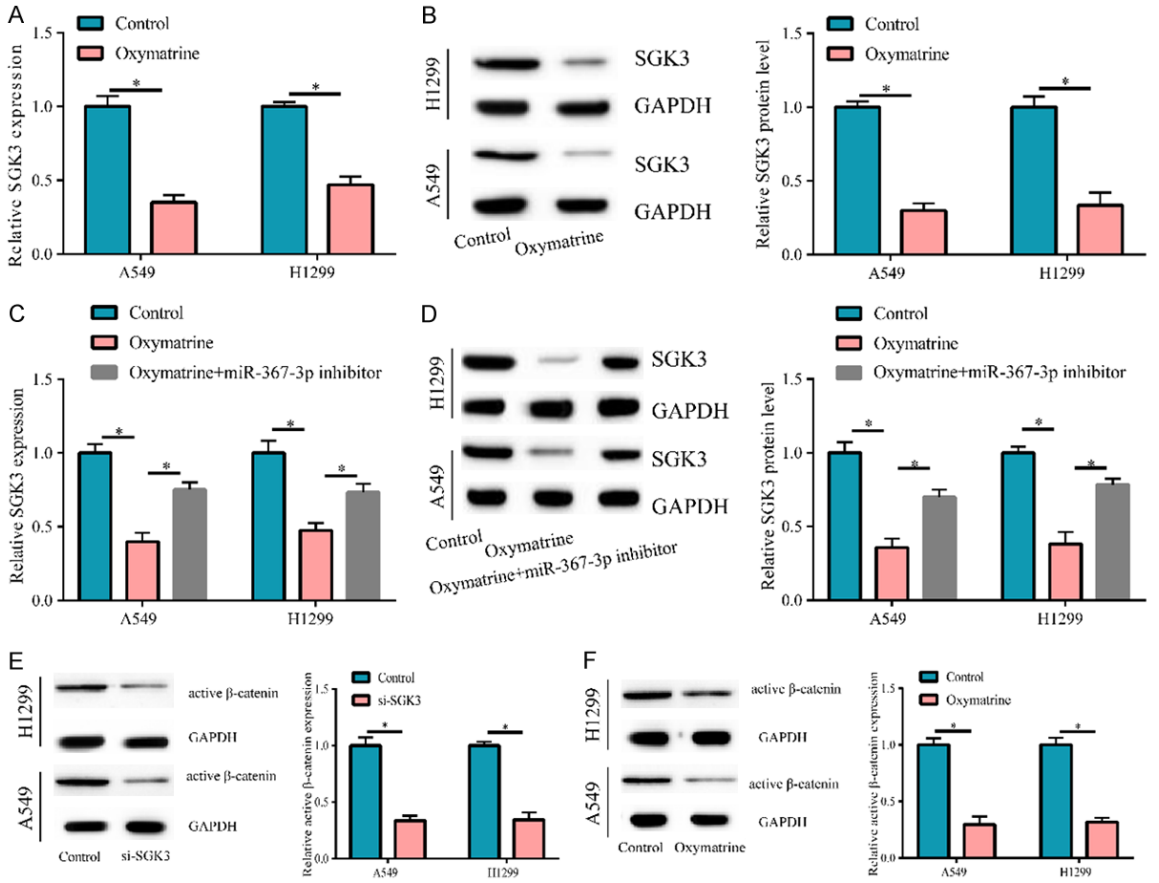

Figure 4. *SGK3* was down-regulated by OM. When cells treated with OM, the mRNA and protein level of SGK3 was reduced (A, B), but partly reversed by downregulating miR-367-3p expression (C, D). (E) After transfecting with si-SGK3, the active β-catenin expression was decreased. (F) When cells treated with OM, the active β-catenin expression was attenuated. *(*P < 0.05).*

transfection of miR-367-3p mimics, mRNA, and protein expressions of *SGK3* were notably decreased, which also suggested the target actions of miR-367-3p on *SGK3* (**Figure 3C**, **3D**).

SGK3 was down-regulated by OM

Since OM increased miR-367-3p expression, we investigated whether OM decreased *SGK3* expression. Therefore, after cell treatment using OM (50 μM), *SGK3* expression was also detected, and the results suggested that mRNA and protein expressions of *SGK3* in OM-treated cells were remarkably reduced versus the control group (**Figure 4A**, **4B**). Meanwhile, we found that the downregulation of miR-367-3p could partly reverse *SGK* expression, which was decreased by OM (**Figure 4C**, **4D**). Thereby, OM could regulate *SGK3* via miR-367-3p. Furthermore, we detected that the active β-catenin expression was faded by downregulating *SGK3* (**Figure 4E**) and that OM could also inhibit the expression of active β-catenin (**Figure 4F**).

Roles of OM/miR-367-3p/SGK3 axis

For an in-depth exploration, an experiment was carried out and uncovered that after cell treatment using OM, the inhibiting effects of OM on cell migration and proliferation were partially recovered by the downregulation of miR-367-3p in A 549 and H1299 cell lines (**Figure 5A-E**). To explore the possible mechanism of action of miR-367-3p, both miR-367-3p and SGK3 expressions were upregulated (**Figure 5F**, **5G**) and the cell migration and proliferation in each group were also detected. The results indicated that an upregulation of SGK3 partially reversed the inhibition effects of upregulated miR-367-3p on NSCLC cell migration and proliferation, suggesting that miR-367-3p might exert its

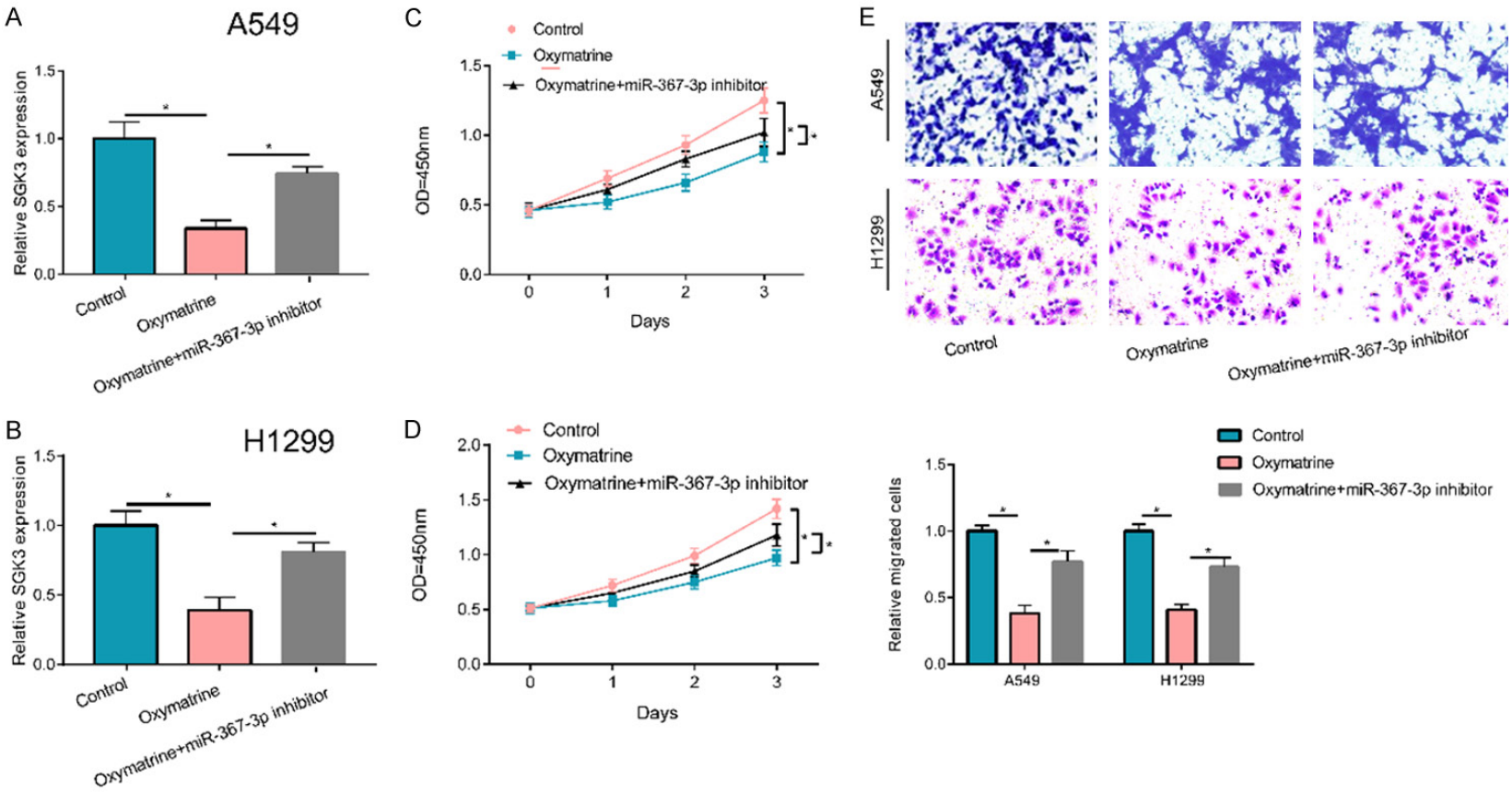
A
A549
Relative SGK3 expression
1.5
1.0
0.5
0.0
*
*
Control
Oxymatrine
Oxymatrine+miR-367-3p inhibitor
B
H1299
Relative SGK3 expression
1.5
1.0
0.5
0.0
*
*
Control
Oxymatrine
Oxymatrine+miR-367-3p inhibitor
C
Control
Oxymatrine
Oxymatrine+miR-367-3p inhibitor
OD=450nm
1.5
1.0
0.5
0.0
0
1
2
3
Days
*
*
D
Control
Oxymatrine
Oxymatrine+miR-367-3p inhibitor
OD=450nm
2.0
1.5
1.0
0.5
0.0
0
1
2
3
Days
*
*
E
A549
H1299
Control
Oxymatrine
Oxymatrine+miR-367-3p inhibitor
Relative migrated cells
1.5
1.0
0.5
0.0
*
*
*
*
A549
H1299
Control
Oxymatrine
Oxymatrine+miR-367-3p inhibitor

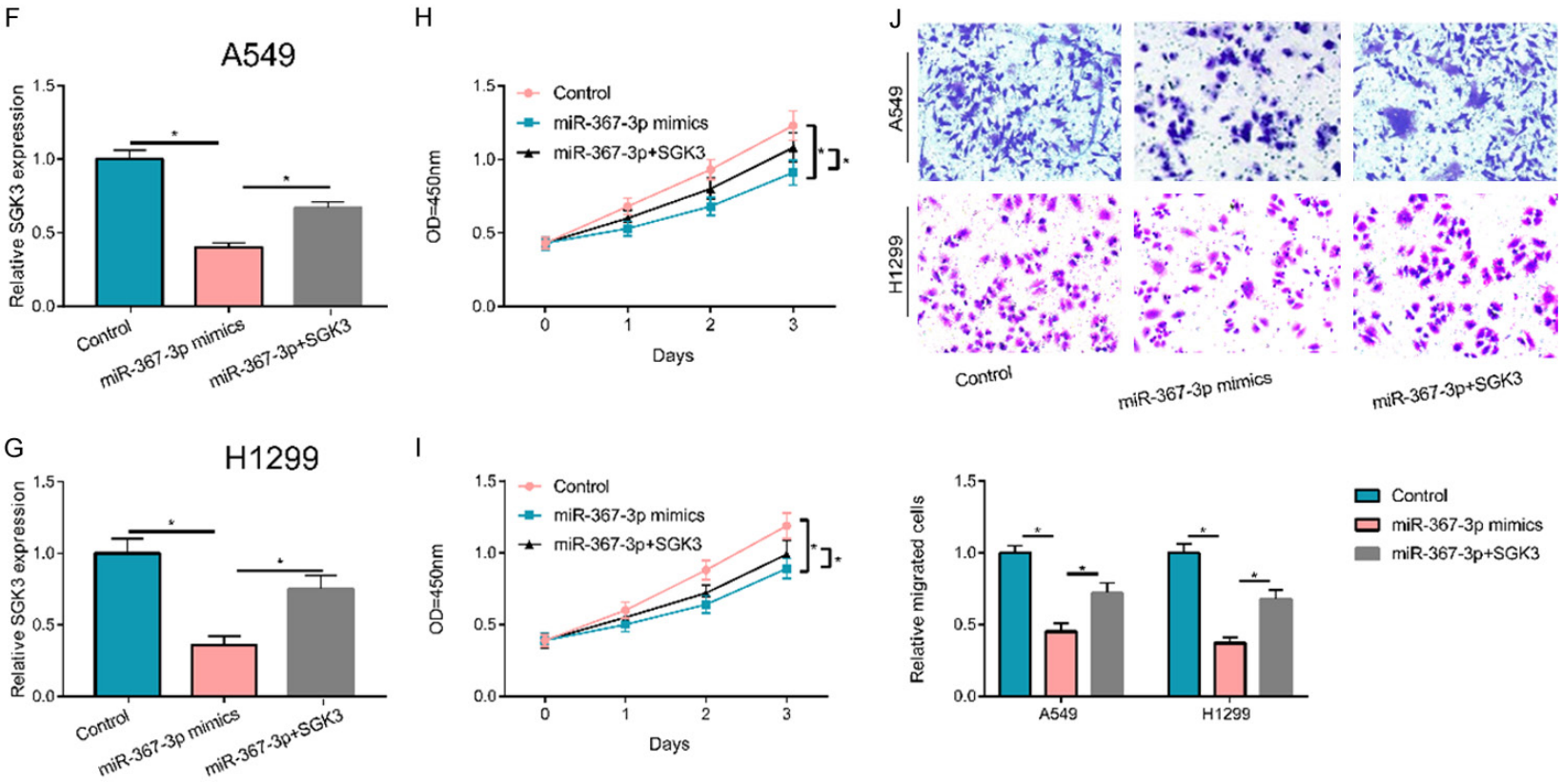

Figure 5. Roles of OM/miR-367-3p/*SGK3* axis. A, B. The negative effect of OM on the expression of *SGK3* could be partly reversed by miR-367-3p inhibitor. C-E. Suppression effects of OM on cell proliferation and migration partially relieved by the downregulation of miR-367-3p. F, G. The up-regulated miR-367-3p inhibited the expression of *SGK3*, but partly reversed by transfecting *SGK3* overexpression plasmid. H-J. Suppression on cell migration and proliferation by miR-367-3p mimics partially reversed by the upregulation of *SGK3*. *(*P* < 0.05*)*.

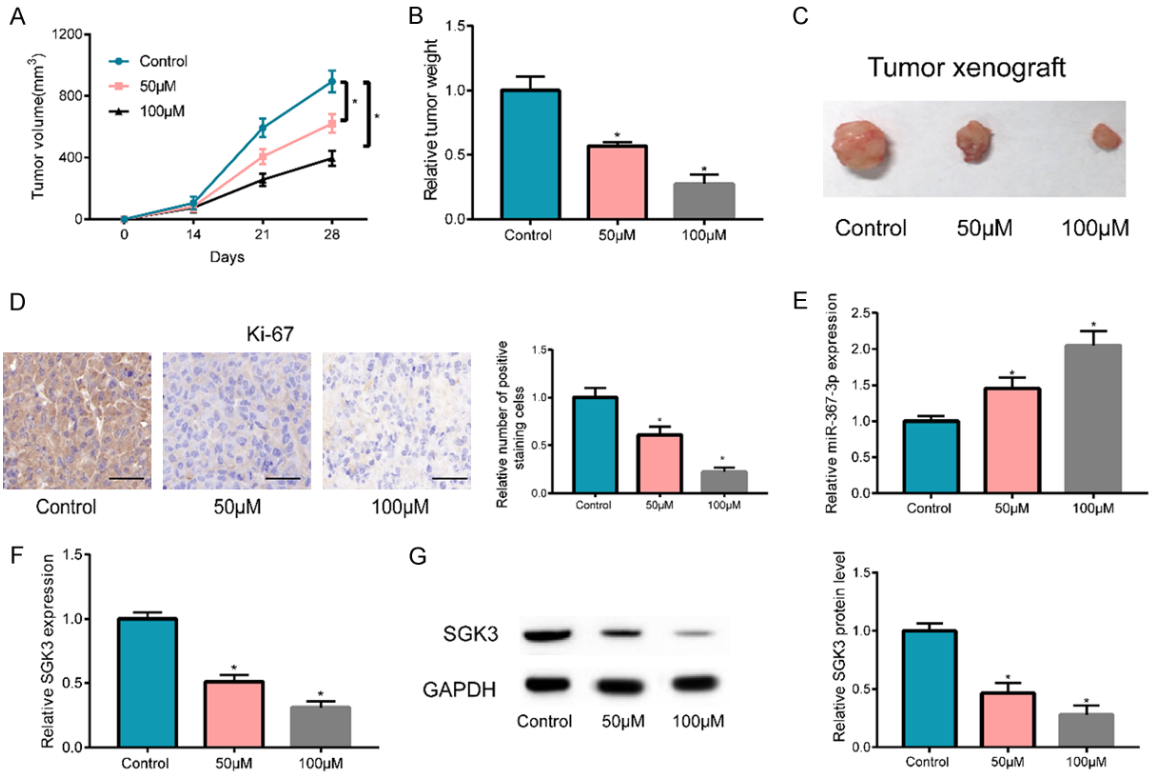

Figure 6. OM inhibited tumor growth *in vivo*. A-C. In nude mice, tumor growth (tumor volume, tumor weight and the tumor size) was inhibited by OM *in vivo* and has a concentration dependent effect. D. Immunohistochemical assay revealed that the relative number of Ki67 positive expression cells in OM-treated group were considerably lower versus the control group in certain dose-dependent pattern. E. miR-367-3p expression in tumors of OM-treated group was considerably higher versus control group. F, G. The *SGK3* expression in tumor of OM-treated group was notably lower relative to control group. *(*P* < 0.05*).*

roles by targeting SGK3 (**Figure 5H-J**). Therefore, OM might play its role through miR-367-3p/SGK3 pathway in NSCLC.

OM inhibited tumor growth in vivo

For the detection of the effects of OM on tumor formation and growth of NSCLC cells *in vivo*, A549 cells were transfected into nude mice of the OM-treated group (50 and 100 μM) and the control group (untreated group) by subcutaneous injection. Transfection started seven days post injection, and a seven-day interval was used for the measurement of tumor size until 28 days had passed. The findings revealed that both tumor volume (**Figure 6A**) and final tumor weight and size (**Figure 6B**, **6C**) of the control group from 14 days onward were significantly higher, relative to the OM-treated group. These findings uncovered that OM restrained tumor formation and growth of NSCLC cells *in vivo* in a certain concentration-dependent manner. To signify cell proliferation in tumors, an immunohistochemical method was utilized to detect Ki67 expression in tumors of each group. The results objectivized that the control group, the low-dose OM group, and the high-dose OM group had a lower Ki67 positive expression in cells and a lower positive staining degree in tumor tissues, in turn, suggesting that cell proliferation in tumors was somewhat slowed down by the OM treatment (**Figure 6D**). Finally, miR-367-3p expression in the tumor was detected and the results showed that OM-treated group had a significantly higher miR-367-3p expression (**Figure 6E**). We also detected that mRNA and protein levels of *SGK3* were considerably reduced in the OM-treated group (**Figure 6F**, **6G**).

Discussion

At present, lung cancer is mainly treated using surgery, radiotherapy, chemotherapy, and targeted therapy; however, these therapeutic methods also have great side effects and com-

promise the patients' quality of life. Characterized by less and less toxic side effects, convenient accessibility, low cost, sensitivity improvement of radiotherapy and chemotherapy, enhancement of patients' immunity, a longer life span, and a lower probability of drug resistance, traditional Chinese medicines greatly remedy the weaknesses of the existing tumor treatment drugs [13]. From the perspective of OM as a traditional Chinese herb, the present study revealed that OM considerably inhibited NSCLC cell migration and proliferation in a certain concentration-dependent manner; however, little is known on its possible mechanism.

Currently, although traditional Chinese medicine against lung cancer has become a focus of attention, its mode of anti-tumor action is still unclear. Studies in recent years have showed that miRNA is strongly associated with the anti-tumor action of active ingredients in traditional Chinese medicine, and miRNAs may be involved as an oncogene and cancer suppressor gene [14, 15]. Therefore, research has been performed at the miRNA level. The mode of action for anti-tumor effects of active ingredients in traditional Chinese medicine is of great significance. miRNA, an endogenous noncoding short interfering RNA molecule with approximate 18~24 bases, is generated by Dicer enzyme, by shearing and processing a single stranded RNA with a hairpin structure and approximately 70 bases. The expression level of mRNA is regulated to affect the efficiency of protein translation and enhance or suppress tumor development by matching with mRNA 3' untranslated region (3'-UTR) and by binding to AGO proteins to generate the core elements of the RNA-induced silencing complex [16]. As reported before [17], there was a change in miRNA expression in ginsenoside Rh2 treated group versus the control group in human NSCLC A549 cells using miRNA microarray analysis, and the results showed 44 upregulated miRNAs and 24 downregulated miRNAs, with miR-148a presenting the most significant upregulation and miR-424 presenting the most notable downregulation. A miRNA target gene prediction software found that these target genes were associated with cell differentiation, proliferation, and apoptosis. Since previous studies have revealed that miR-367-3p is a cancer suppressor gene, we raised the question on whether OM affects miR-367-3p expression. Therefore, miR-367-3p expression was detected in OM-treated NSCLC cells, and the findings uncovered that miR-367-3p expression was notably increased and an upregulated miR-367-3p significantly suppressed cell proliferation and migration, indicating that OM exerted its roles by suppressing miR-367-3p expression.

Serum and glucocorticoid regulated kinase 3 (*SGK3*), a newly discovered PI3K downstream signal molecule in recent years, may be associated with a cell phosphorylation cascade reaction. Its expression can promote tumor cell proliferation, invasion, and metastasis; thus, *SGK3* is crucial for differentiation, survival, and material transport. *SGK3* is a member of SGK family associated with the occurrence of multiple human tumors [18, 19]. As reported before, SGK family (including *SGK3*) participates in the malignant transformation of cells, suggesting its vital role in tumor occurrence and development [20]. Further studies found that *SGK3* is a key factor of the promotion of tumor occurrence and development in AKT-independent PI3K/mTOR signal transduction pathway [21]. In addition, a study demonstrated that *SGK3* is crucial for the occurrence and development of BRAF mutant malignant melanoma [22]. In this study, both bioinformatics analysis and the dual luciferase reporter gene experiment found that *SGK3* was a possible target gene of miR-367-3p and in-depth verification proved a lower *SGK3* expression via upregulation of miR-367-3p. We found that OM also downregulated *SGK3* expression, which could be partly reversed by the downregulation of miR-367-3p. Additionally, we found that miR-367-3p exerted its roles by regulating *SGK3*, while OM played a role in promoting miR-367-3p expression. Therefore, we demonstrated that OM might take part in the progression of NSCLC by regulating *SGK3* via miR-367-3p.

As reported before, SGK3 could enhance the phosphorylation of GSK-3β on Thr9 (inactivated) to inhibit GSK-3β-mediated degradation of β-catenin [23]. Another study confirmed that down-regulating SGK3 decreases the level of active β-catenin and then attenuates cell migration and invasion [24]. In this study, we also found that, after down-regulating SGK3, the expression of β-catenin was also reduced

in NSCLC cells. Considering that OM decreased SGK3 expression, we further verified whether OM could also inhibit β-catenin activation. As results have shown, when NSCLC cells were treated with OM, β-catenin was inactive. Thus, OM may exert its functions through promoting miR-367-3p expression to downregulate *SGK3* expression and then inactive β-catenin.

To further verify the effects of OM on NSCLC, a tumor-bearing nude mice experiment was used for detecting the roles of OM in tumor growth and signified that OM notably restrained tumor growth, and both tumor volume and mass in OM-treated group were considerably lower, relative to the control group. Moreover, an immunohistochemistry experiment detected that Ki67 expression in tumor tissues of OM-treated group was significantly lower versus the control group. In addition, a significantly higher miR-367-3p expression and a remarkably lower *SGK3* expression in OM-treated group suggested that the OM/miR-367-3p/*SGK3* axis played a certain role in inhibiting the growth of tumor cells and tumors.

In conclusion, this study revealed and explored the roles of OM in NSCLC and its possible mechanism of action, first supposing that OM might promote miR-367-3p expression, downregulate *SGK3* expression, and then inhibit active β-catenin expression during the procedure of NSCLC. This not only enriches the NSCLC research contents, but also provides a novel theoretical foundation and therapeutic target for its prevention and cure.

Acknowledgements

Fujian Provincial Natural Science Foundation [No. 2018J01243].

Disclosure of conflict of interest

None.

Address correspondence to: Xing Lin, Department of Thoracic Surgery, Fujian Provincial Hospital, NO. 134, East Street, Fuzhou 350001, Fujian Province, China. E-mail: zxcvys1@163.com

References

[1] Park SJ, Lee CS and Chung SS. Surgical results of metastatic spinal cord compression (MSCC) from non-small cell lung cancer (NSCLC): analysis of functional outcome, survival time, and complication. Spine J 2016; 16: 322-328.

[2] Lee G, Gardner BK, Elashoff DA, Purcell CM, Sandha HS, Mao JT, Krysan K, Lee JM and Dubinett SM. Elevated levels of CXC chemokine connective tissue activating peptide (CTAP)-III in lung cancer patients. Am J Transl Res 2011; 3: 226-233.

[3] Talbot SG, Estilo C, Maghami E, Sarkaria IS, Pham DK, O-charoenrat P, Socci ND, Ngai I, Carlson D, Ghossein R, Viale A, Park BJ, Rusch VW and Singh B. Gene expression profiling allows distinction between primary and metastatic squamous cell carcinomas in the lung. Cancer Res 2005; 65: 3063-3071.

[4] Wu C, Huang W, Guo Y, Xia P, Sun X, Pan X and Hu W. Oxymatrine inhibits the proliferation of prostate cancer cells in vitro and in vivo. Mol Med Rep 2015; 11: 4129-4134.

[5] Wu XS, Yang T, Gu J, Li ML, Wu WG, Weng H, Ding Q, Mu JS, Bao RF, Shu YJ, Cao Y, Wang XA, Ding QC, Dong P, Xie SF and Liu YB. Effects of oxymatrine on the apoptosis and proliferation of gallbladder cancer cells. Anticancer Drugs 2014; 25: 1007-1015.

[6] Lin B, Li D and Zhang L. Oxymatrine mediates Bax and Bcl-2 expression in human breast cancer MCF-7 cells. Pharmazie 2016; 71: 154-157.

[7] Wang B, Han Q and Zhu Y. Oxymatrine inhibited cell proliferation by inducing apoptosis in human lung cancer A549 cells. Biomed Mater Eng 2015; 26 Suppl 1: S165-172.

[8] Yoo B, Meka N, Sheedy P, Billig AM, Pantazopoulos P and Medarova Z. MicroRNA-710 regulates multiple pathways of carcinogenesis in murine metastatic breast cancer. PLoS One 2019; 14: e0226356.

[9] Nie H, Xie X, Zhang D, Zhou Y, Li B, Li F, Li F, Cheng Y, Mei H, Meng H and Jia L. Use of lung-specific exosomes for miRNA-126 delivery in non-small cell lung cancer. Nanoscale 2020; 12: 877-887.

[10] Yang T, Tian S, Wang L, Wang Y and Zhao J. MicroRNA-367-3p overexpression represses the proliferation and invasion of cervical cancer cells through downregulation of SPAG5-mediated Wnt/beta-catenin signaling. Clin Exp Pharmacol Physiol 2020; 47: 687-695.

[11] Rosas Plaza X, van Agthoven T, Meijer C, van Vugt MATM, de Jong S, Gietema JA and Looijenga LHJ. miR-371a-3p, miR-373-3p and mir-367-3p as serum biomarkers in metastatic testicular germ cell cancers before, during and after chemotherapy. Cells 2019; 8: 1221.

[12] Liu X, Zheng J, Xue Y, Yu H, Gong W, Wang P, Li Z and Liu Y. PIWIL3/OIP5-AS1/miR-367-3p/CEBPA feedback loop regulates the biological behavior of glioma cells. Theranostics 2018; 8: 1084-1105.

[13] Zhang Y, Zhang GB, Xu XM, Zhang M, Qu D, Niu HY, Bai X, Kan L and He P. Suppression of growth of A549 lung cancer cells by waltonitone and its mechanisms of action. Oncol Rep 2012; 28: 1029-1035.
[14] Ye MX, Zhao YL, Li Y, Miao Q, Li ZK, Ren XL, Song LQ, Yin H and Zhang J. Curcumin reverses cis-platin resistance and promotes human lung adenocarcinoma A549/DDP cell apoptosis through HIF-1alpha and caspase-3 mechanisms. Phytomedicine 2012; 19: 779-787.
[15] Zhang W, Bai W and Zhang W. MiR-21 suppresses the anticancer activities of curcumin by targeting PTEN gene in human non-small cell lung cancer A549 cells. Clin Transl Oncol 2014; 16: 708-713.
[16] Chandra V, Kim JJ, Mittal B and Rai R. MicroRNA aberrations: an emerging field for gallbladder cancer management. World J Gastroenterol 2016; 22: 1787-1799.
[17] An IS, An S, Kwon KJ, Kim YJ and Bae S. Ginsenoside Rh2 mediates changes in the microRNA expression profile of human non-small cell lung cancer A549 cells. Oncol Rep 2013; 29: 523-528.
[18] Wang H, Huang F, Zhang Z, Wang P, Luo Y, Li H, Li N, Wang J, Zhou J, Wang Y and Li S. Feedback activation of SGK3 and AKT contributes to rapamycin resistance by reactivating mTORC1/4EBP1 axis via TSC2 in breast cancer. Int J Biol Sci 2019; 15: 929-941.
[19] Cao H, Xu Z, Wang J, Cigliano A, Pilo MG, Ribback S, Zhang S, Qiao Y, Che L, Pascale RM, Calvisi DF and Chen X. Functional role of SGK3 in PI3K/Pten driven liver tumor development. BMC Cancer 2019; 19: 343.
[20] Bruhn MA, Pearson RB, Hannan RD and Sheppard KE. Second AKT: the rise of SGK in cancer signalling. Growth Factors 2010; 28: 394-408.
[21] Bruhn MA, Pearson RB, Hannan RD and Sheppard KE. AKT-independent PI3-K signaling in cancer - emerging role for SGK3. Cancer Manag Res 2013; 5: 281-292.
[22] Scortegagna M, Lau E, Zhang T, Feng Y, Sereduk C, Yin H, De SK, Meeth K, Platt JT, Langdon CG, Halaban R, Pellecchia M, Davies MA, Brown K, Stern DF, Bosenberg M and Ronai ZA. PDK1 and SGK3 contribute to the growth of BRAF-mutant melanomas and are potential therapeutic targets. Cancer Res 2015; 75: 1399-1412.
[23] Voulgari A and Pintzas A. Epithelial-mesenchymal transition in cancer metastasis: mechanisms, markers and strategies to overcome drug resistance in the clinic. Biochim Biophys Acta 2009; 1796: 75-90.
[24] Kong X, Liu F and Gao J. MiR-155 promotes epithelial-mesenchymal transition in hepatocellular carcinoma cells through the activation of PI3K/SGK3/beta-catenin signaling pathways. Oncotarget 2016; 7: 66051-66060.